Figure S1

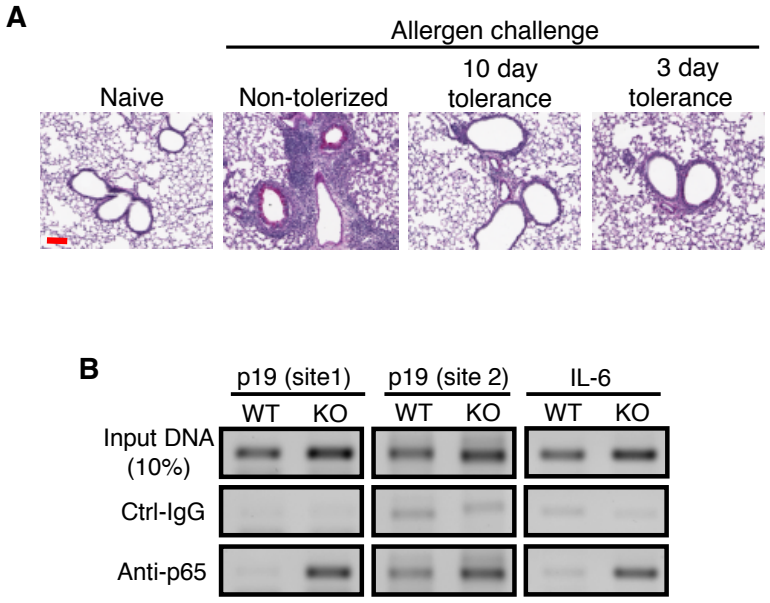
A
Allergen challenge
Naive
Non-tolerized
10 day tolerance
3 day tolerance
B
p19 (site1)
p19 (site 2)
IL-6
WT
KO
WT
KO
WT
KO
Input DNA (10%)
Ctrl-IgG
Anti-p65

Figure S2

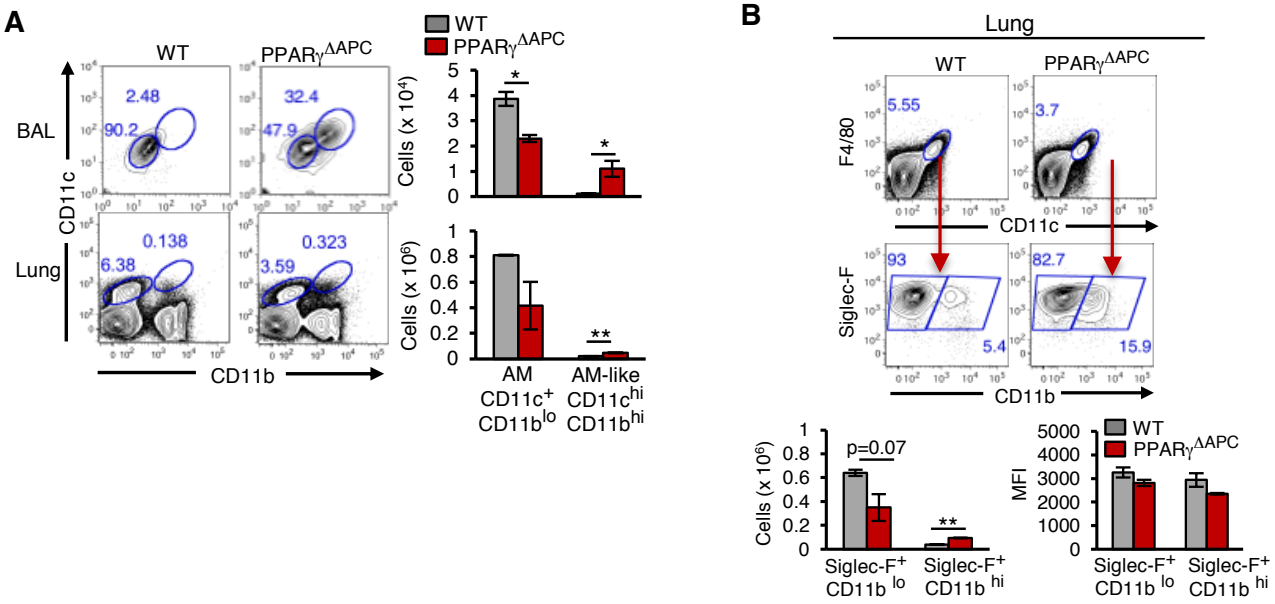
A
WT
PPARγ^ΔAPC
BAL
Lung
CD11c
CD11b
2.48
90.2
32.4
47.9
0.138
6.38
0.323
3.59
Cells (x 10⁴)
Cells (x 10⁶)
AM
CD11c+ CD11blo
AM-like
CD11chi CD11bhi
B
Lung
F4/80
Siglec-F
5.55
3.7
93
5.4
82.7
15.9
p=0.07
MFI
Siglec-F+ CD11b lo
Siglec-F+ CD11b hi

Figure S3

Lane 1:Naïve-WT
Lane 2:OVA Tol-WT
Lane 3:Naïve-WT+RSG
Lane 4:Naïve-PPARγ$^{\Delta APC}$
Lane 5:OVA Tol-PPARγ$^{\Delta APC}$

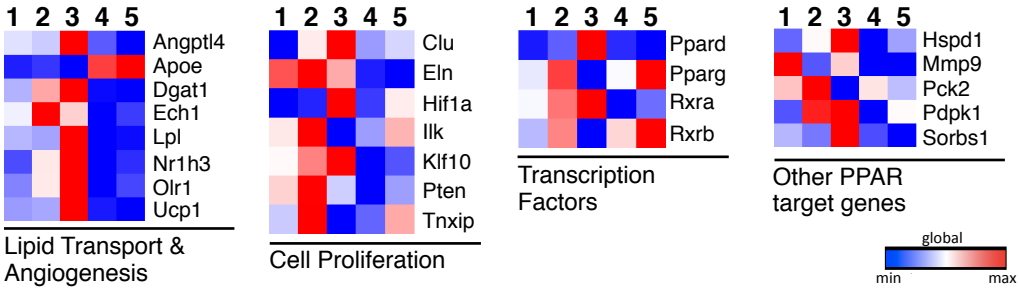

Figure S4

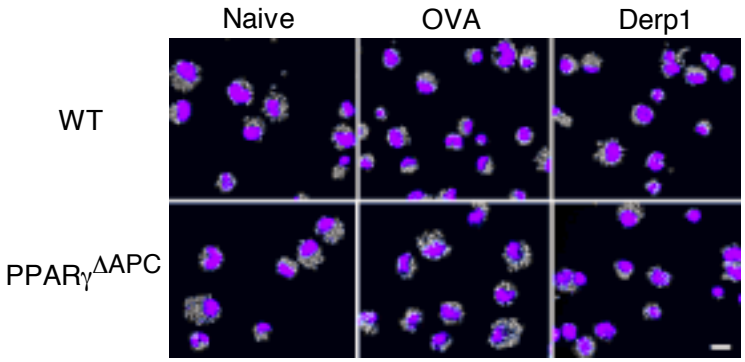

Figure S5

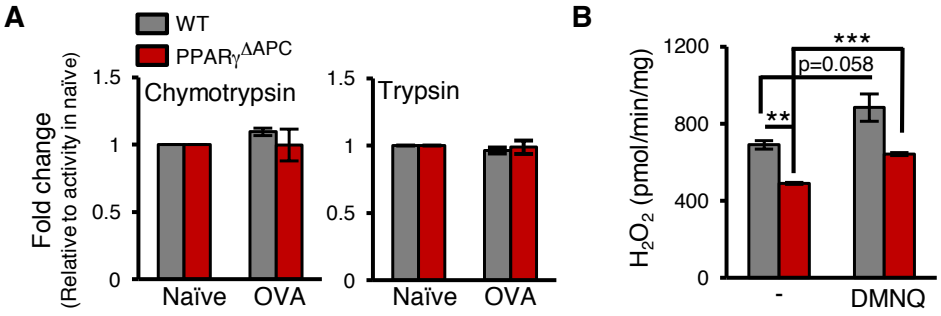
A
WT
PPARγ^ΔAPC
Fold change
(Relative to activity in naïve)
Chymotrypsin
Trypsin
1.5
1
0.5
0
Naïve
OVA
B
H2O2 (pmol/min/mg)
1200
800
400
0
***
p=0.058
**
-
DMNQ

Figure S6

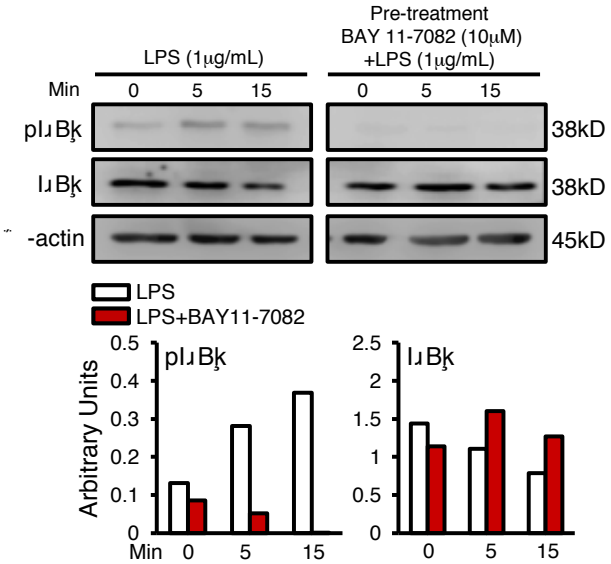
Pre-treatment
BAY 11-7082 (10μM)
+LPS (1μg/mL)
LPS (1μg/mL)
Min
0
5
15
0
5
15
pIκBα
IκBα
β-actin
38kD
38kD
45kD
LPS
LPS+BAY11-7082
Arbitrary Units
pIκBα
IκBα
0.5
0.4
0.3
0.2
0.1
0
2.5
2
1.5
1
0.5
0
Min 0 5 15
0 5 15

Supplemental Figure Legends

Figure S1, related to Figure 1

(A) PPAR$\gamma^{fl/fl}$ (WT) mice were tested for induction of tolerance using 3-day or 10 day tolerance models as described under methods. 24 hr after last challenge, PAS staining was performed on lung histology sections acquired from indicated conditions. Scale bar, 100 μm and magnification 20X, n=2. (B) ChIP assay of p19 and IL-6 promoters in $CD11c^+$ cells isolated from WT mice aerosolized with the 10-day tolerance protocol, using anti-p65 and control antibodies.

Figure S2, related to Figure 1

(A) Flow cytometry-based identification (left) and enumeration (right) of AMs ($CD11c^+CD11b^{lo}$) and AM-like ($CD11c^{hi}CD11b^{hi}$) cells in BAL and lung of naïve WT and PPAR$\gamma^{\Delta APC}$ mice. (B) Expression of Siglec-F and CD11b (top) and enumeration of different subpopulations (bottom) on gated $CD11c^+F4/80^+$ cells from lungs of naïve WT and PPAR$\gamma^{\Delta APC}$ mice. Numbers next to the gates, inside the flow diagram indicate the frequency of the respective subpopulation. Data shown are representative of two independent experiments and shown as mean ± SD. **p< 0.01, *p<0.05.

Figure S3, related to Figure 1

Heat map representation of PPAR target array data of the indicated genes (clustered based on function) from $CD11c^+$ APCs from naïve (Lane 1), tolerized

(Lane 2) , *ex-vivo* RSG-treated WT (Lane 3) along with naïve (Lane 4) and tolerized PPAR$\gamma^{\Delta APC}$ (Lane 5) mice are shown.

Figure S4, related to Figure 3

Representative surface rendering images of CD11c^{+} cells from WT and PPAR$\gamma^{\Delta APC}$ mice (subjected to indicated treatments) stained with mitochondrial marker Tom20 (green), actin (red) and DAPI (blue). 3D rendering (white) was performed to measure mitochondrial volume using Imaris software (Bitplane). Scale bar, 10 μm and magnification 60X, n=2.

Figure S5, related to Figure 4

(**A**) Lung CD11c^{+} APCs sorted from naïve and/or OVA-exposed WT and PPAR$\gamma^{\Delta APC}$ mice (one hr after the last exposure to allergen) were analyzed for Chymotyrpsin-and Trypsin-like protease activity. Data shown are represented as fold change relative to activity measured in naïve CD11c^{+} APCs. (**B**) H_2O_2 generation was assessed in OVA-exposed lung CD11c^{+} APCs in the presence or absence of DMNQ (200 μM). Cells were cultured for 1 hr at 37^0C. All data shown are representative of two independent experiments and shown as mean ± SEM. ***p< 0.001, **p<0.01.

Figure S6, related to Figure 5

Phospho IκBa (pIκBa) and IκBa levels in total cell extract from splenic cells pre-treated with either vehicle or BAY11-7082 (10 mM) and stimulated with LPS (1 mg/mL) for indicated time points. Expression of β-actin is shown as loading control and densitometric quantification represented.